


 Cite this: *RSC Adv.*, 2025, 15, 38024

# A rapid, metal-free synthesis of amino- and hydroxyphenanthrenes with tunable photophysical properties

Hamza Enesi Ozomaris and Victor K. Outlaw \*

Here we report a general, metal-free strategy for the regioselective synthesis of amino- and hydroxyphenanthrenes from 1- and 2-naphthaldehydes. The sequence employs an *E*-selective Wittig olefination, followed by a regioselective Houben–Hoesch annulation, enabling access to 1- and 4-substituted amino- and hydroxyphenanthrenes in moderate yields. The method tolerates diverse substitution patterns and proceeds without the need for precious metal catalysts or elaborate precursors. Substituents introduced *via* this approach significantly modulate the absorption and emission properties of the resulting phenanthrenes, underscoring the utility of the method for generating phenanthrene-based materials with tunable photophysical behavior.

 Received 29th August 2025  
 Accepted 6th October 2025

DOI: 10.1039/d5ra06485f

[rsc.li/rsc-advances](https://rsc.li/rsc-advances)

Amino- and hydroxy-substituted phenanthrenes are valuable scaffolds in a variety of applications,<sup>1</sup> including optoelectronic materials,<sup>2–8</sup> imaging agents,<sup>4,5</sup> ligands,<sup>9,10</sup> natural products, and therapeutics (Fig. 1).<sup>11–17</sup> Given this broad utility, considerable effort has been devoted to the development of synthetic strategies for amino- and hydroxyphenanthrene analogs,<sup>18–29</sup> including several notable examples employing electrophilic aromatic substitution (EAS) as the final annulation step (Scheme 1). DeShong and co-workers reported a route initiated by arylsiloxane cross-coupling to afford biaryl aldehydes, followed by Wittig homologation, Jones oxidation, and Friedel–Crafts annulation to phenanthrene precursors of the allocholicinoid natural product family.<sup>18</sup> Dash and co-workers described a vinyl trifluoroborate coupling of 1-bromo-2-naphthaldehyde, followed by indium-mediated Barbier allylation, Dess–Martin oxidation, and ring-closing metathesis to generate 1-hydroxyphenanthrenes.<sup>19</sup> De Mesmaeker employed a Suzuki cross-coupling of iodo-substituted phenylacetic acids, followed by amide coupling with secondary amines and triflic anhydride-mediated cyclization to access aminophenanthrenes.<sup>20</sup> While these strategies demonstrate the diverse chemical approaches to phenanthrene synthesis, they also illustrate common limitations, including reliance on complex starting materials, precious metal catalysts, and multiple discrete steps to obtain a single amino- or hydroxyphenanthrene isomer.

Here we report a general, metal-free, and expedient method for the synthesis of 1-amino-, 4-amino-, 1-hydroxy-, and 4-hydroxyphenanthrenes directly from 1- and 2-naphthaldehydes (Scheme 1d). This approach combines an *E*-selective Wittig

olefination with a regioselective Houben–Hoesch annulation in a streamlined two-step sequence, enabling rapid scaffold diversification without the need for precious metal catalysts or elaborate precursors.

Given the importance of specifically tuned electronic and photophysical properties for the performance of phenanthrene-based materials, we further demonstrate that substitution patterns introduced by our method are able to modulate the absorption and emission profiles of the resulting scaffolds. These findings not only underscore the synthetic versatility of the approach but also establish its utility as a platform for the development of next-generation phenanthrene-based materials.

We envisioned a two-step route to access the desired phenanthrene scaffolds. In the first step, olefination of naphthaldehydes (**1**) with fumaronitrile (**2**) or diethyl fumarate (**3**) would furnish naphthalenylmethylene succinonitrile (**4**) or

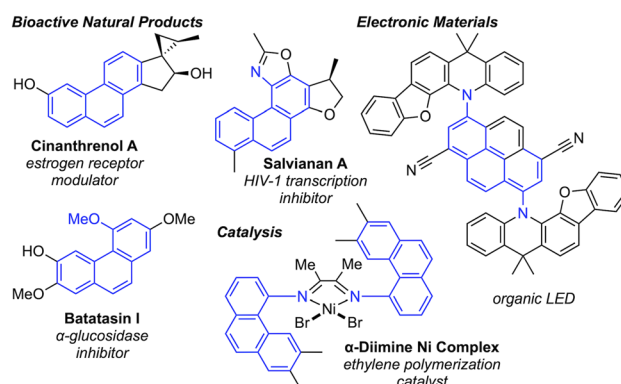
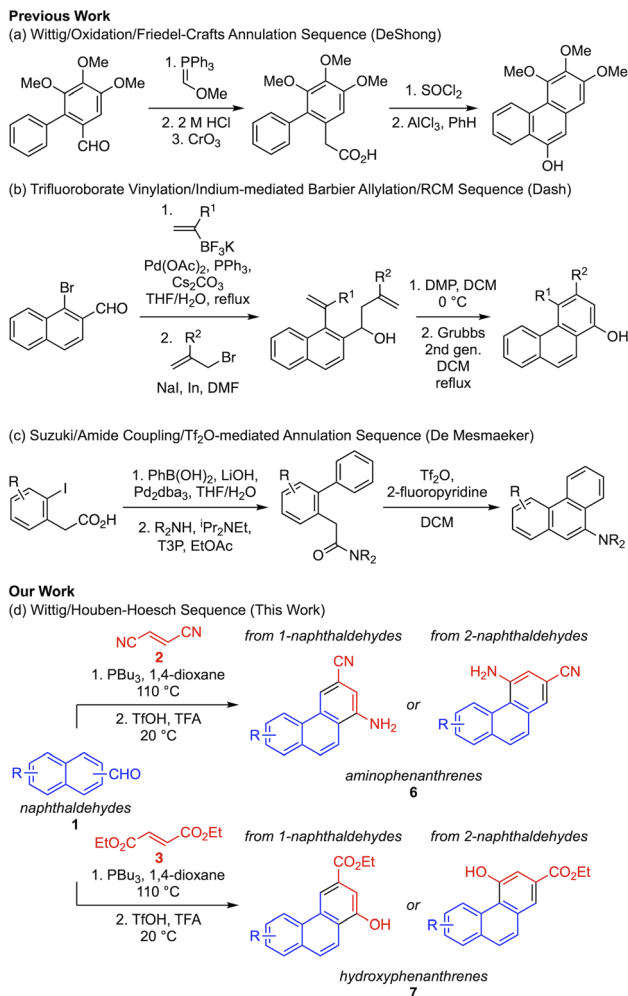


Fig. 1 Representative amino- and hydroxyphenanthrene derivatives in natural products, therapeutics, electronic materials, and catalysts.

Department of Chemistry, University of Missouri, Columbia, Missouri, 65211, USA.  
 E-mail: victoroutlaw@missouri.edu





**Scheme 1** (a–c) Representative strategies for the synthesis of either amino- or hydroxy-substituted phenanthrenes. (d) Our envisioned divergent route to both amino- and hydroxyphenanthrenes from naphthaldehyde precursors.

succinate (5) intermediates, respectively. Subsequent annulation *via* intramolecular Houben–Hoesch reaction would yield aminophenanthrenes (6) and hydroxyphenanthrenes (7). This

strategy allows for regioselective introduction of amino or hydroxy substituents at the 1- and 4-positions of the phenanthrene core.

Achieving high *E*-selectivity in the olefination step was critical to the success of the envisioned synthetic route. To this end, we evaluated both Wittig and Horner-Wadsworth-Emmons conditions. The stereoselectivity of these olefination reactions is known to depend strongly on the steric and electronic properties of the aldehyde substrate. For example, a one-pot, three component Wittig reaction of pyrrole-3-aldehydes with fumaronitrile and tributylphosphine has been reported to proceed with high *E*-selectivity.<sup>30</sup> In contrast, analogous reactions with benzaldehyde favored formation of the undesired *Z*-isomer, necessitating the use of the Still-Gennari modification of the Horner-Wadsworth-Emmons (HWE-Still) reaction to obtain predominantly *E*-isomer.<sup>31</sup>

To establish optimal conditions for *E*-selective olefination of naphthaldehydes, we screened a series of Wittig and HWE protocols using naphthaldehyde **1a** as a model substrate (Table 1). Under Wittig conditions (tributylphosphine, **2**, 110 °C) olefination proceeded in 81% yield with a 4 : 1 mixture of *E*/*Z* isomers. This result contrasts with the reported *Z*-selectivity for Wittig olefination of benzaldehydes.<sup>31</sup> HWE conditions (diethyl phosphite, NaH, **2**, 20 °C), led to a diminished 1 : 2 *E*/*Z* ratio favoring the undesired *Z*-isomer in 71% yield. In contrast, the HWE-Still protocol (bis(trifluoroethyl)phosphite, NaH, **2**, –78 °C) afforded a 6 : 1 *E*/*Z* mixture in 76% yield, consistent with the selectivity reported for benzaldehydes under similar conditions.

For all three cases, the *E* and *Z* isomers of **4a** proved inseparable by chromatographic or crystallization methods. To circumvent this limitation and to streamline the synthesis, we adopted a two-step protocol in which the crude olefination product was carried forward directly into the annulation step. This approach minimized purification steps and enabled more rapid access to amino- and hydroxy-substituted phenanthrenes.

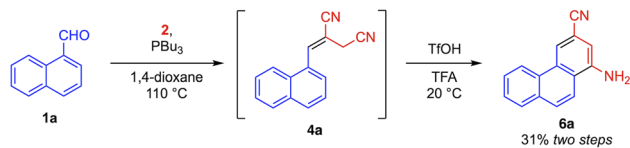
To initiate the two-step strategy, the Wittig reaction was selected based on its lower reagent cost, operational simplicity, and greater compatibility with the subsequent Houben–Hoesch annulation compared to HWE-Still reaction. To identify suitable cyclization conditions, crude Wittig product derived from 1-naphthaldehyde **1a** was filtered through a short plug of silica and

**Table 1** Optimization of conditions for *E*-selective olefination of naphthaldehydes

Entry	Reaction	Reagents	Temp. (°C)	Yield (%)	<i>E</i> / <i>Z</i> <sup>a</sup>
1	Wittig	PBU <sub>3</sub> , dioxane	110	81	4 : 1
2	HWE	Diethyl phosphite, NaH, THF	20	71	1 : 2
3	HWE-Still	bis(trifluoroethyl) phosphite, NaH, THF	–78	76	6 : 1

<sup>a</sup> *E*/*Z* values were determined by the ratio of integrated allylic methylene peaks in the crude <sup>1</sup>H NMR spectra.



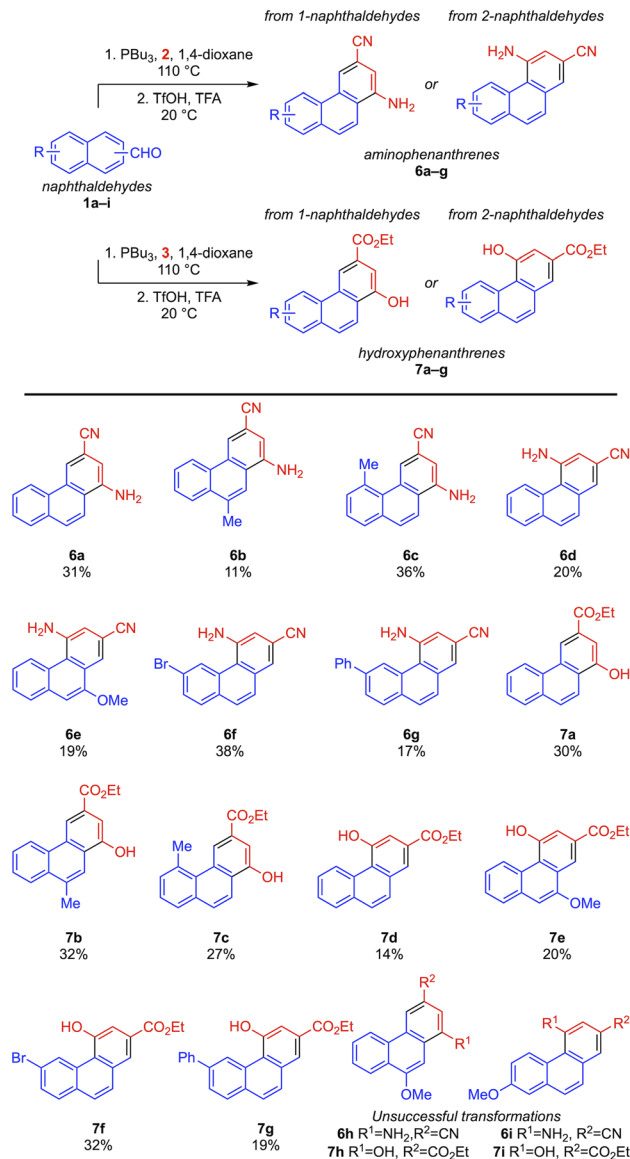


Scheme 2 Two-step sequence for the synthesis of aminophenanthrene **6a**.

treated with various Lewis and Brønsted acids to promote conversion to aminophenanthrene **6a**. Incubation in DCE, AcOH, or TFA failed to effect cyclization. Likewise, treatment with Lewis acids  $\text{ZnCl}_2$ ,  $\text{AlCl}_3$ ,  $\text{Al}(\text{OTf})_3$ , or  $\text{BF}_3 \cdot \text{OEt}_2$  in DCE at 90 °C gave no detectable formation of the desired product (Table S1).  $\text{BF}_3 \cdot \text{OEt}_2$  has been reported to facilitate Houben–Hoesch-type annulations in the synthesis of aminoindoles<sup>30</sup> and aminonaphthalenes.<sup>31</sup> In the latter study, only TfOH in TFA was more effective than  $\text{BF}_3 \cdot \text{OEt}_2$ . Accordingly, treatment of the crude Wittig product with TfOH in TFA furnished 1-amino-3-cyanophenanthrene **6a** in 31% yield (Scheme 2). A proposed mechanism for the transformation (Scheme S1) involves initial TfOH-mediated protonation of the allylic nitrile to generate a reactive nitrilium intermediate, followed by annulation and tautomerization to afford the final phenanthrene product.

To evaluate the scope of the two-step aminophenanthrene synthesis, a panel of 1- and 2-naphthaldehydes (**1a–i**) was subjected to the optimized Wittig and Houben–Hoesch conditions. 1-Naphthaldehydes **1a–c** were converted to 4-aminophenanthrenes **6a–c** in 11–36% isolated yield over two steps, while 2-naphthaldehydes **1d–g** afforded 1-aminophenanthrenes **6d–g** in 17–38% yield (Scheme 3). Notably, annulation occurred exclusively at the 1-position of the naphthalene precursor, with no detectable formation of aminoanthracenes arising from cyclization at the 3-position. The two-step Wittig/Houben–Hoesch protocol proved ineffective for the formation of methoxy-substituted aminophenanthrenes **6h** and **6i**.

To extend the utility of this strategy, we next examined its applicability to the synthesis of hydroxyphenanthrenes. Substituting fumaronitrile with diethyl fumarate in the Wittig reaction provided naphthalenylmethylene succinate intermediates, which were similarly amenable to TfOH-mediated annulation. Under these conditions, 1-naphthaldehydes **1a–c** delivered 4-hydroxyphenanthrenes **7a–c** in 20–32% isolated yield over two steps, and 2-naphthaldehydes **1d–g** afforded 1-hydroxyphenanthrenes **7d–g** in 14–32% yield. As observed for the aminophenanthrenes, annulation occurred regioselectively for the 1-position of the naphthalene ring, and no evidence of anthracene formation *via* cyclization at position 3 was detected. Conversion of methoxy-substituted aldehydes **1h** and **1i** again proved ineffective, with no formation of hydroxyphenanthrene analogs **7h** and **7i** observed. The transformation is proposed to proceed *via* TfOH-mediated activation of the allylic ester, followed by regioselective electrophilic aromatic substitution and tautomerization of the resulting ketone to afford the phenanthrene core (Scheme S2).



Scheme 3 Scope for the two-step synthesis of amino- and hydroxyphenanthrenes directly from naphthaldehydes. Reported yields are isolated yields over two steps.

Assuming that the transition state leading to the carbocation intermediate is the rate-determining step in this EAS-type annulation, the failure of substrates **6h/6i** and **7h/7i** to undergo successful cyclization can be partially attributed to insufficient carbocation stabilization. The position of the electron-donating group relative to the carbocation plays a critical role in stabilizing the transition state and facilitating ring closure. For annulations derived from 1-naphthaldehyde, substituents at positions 3, 6, or 8 are expected to stabilize a developing cation *via* resonance effects (Scheme S3). In contrast, for 2-naphthaldehyde-derived intermediates, electron-donating groups at positions 4, 5, or 7 would favorably stabilize the cation.

In the case of **6h/7h**, the precursor is 4-methoxy-1-naphthaldehyde (**1h**), where the methoxy group is located at



a position (C4) that is poorly positioned for stabilizing the carbocation. Similarly, **6i/7i** arise from 6-methoxy-2-naphthaldehyde (**1i**), where the methoxy substituent at C6 is not optimally positioned to stabilize the cation. In both cases, the electronic effects of the methoxy groups do not contribute effectively to stabilizing the key carbocation intermediate, which may account for the observed lack of annulation under standard conditions.

The exclusive formation of phenanthrenes over the isomeric anthracenes can be attributed to thermodynamic factors. Experimental and computational studies consistently indicate that phenanthrenes are more thermodynamically stable than anthracenes owing to their greater aromatic stabilization and lower standard enthalpies of formation.<sup>32–34</sup> Reported energy differences range from 4.2 to 6.8 kcal mol<sup>-1</sup>, favoring the phenanthrene core. This enhanced stability can also be rationalized using Clar's aromatic sextet theory.<sup>32,35</sup> Phenanthrene contains two aromatic sextets in its outer rings, compared to anthracene which only has one. As a result, phenanthrene benefits from greater resonance stabilization, making it the favored product under thermodynamically controlled conditions. This regioselectivity is also supported by a control experiment in which the 1-position of the naphthalene was blocked by a bromo substituent, preventing cyclization to the phenanthrene. No reaction was observed, suggesting that cyclization at the 3-position to generate the anthracene core is not a viable pathway under the reaction conditions (Scheme S4).

Phenanthrene-based compounds have seen expanded utility in optoelectronic applications, including as thermally activated delayed fluorescence (TADF) emitters,<sup>3</sup> biophysical probes,<sup>4</sup> and pH-responsive fluorophores.<sup>5</sup> In many cases, the tunability of absorption and emission wavelengths is important for function.<sup>6–8</sup> We therefore investigated the effect of substituents on photophysical properties of amino- and hydroxyphenanthrenes accessible by our synthetic method.

In dichloromethane, aminophenanthrene **6d** exhibited absorption and emission maxima at 261 and 408 nm, respectively (Fig. 2A). Introduction of a methoxy group at the 10-position of the aminophenanthrene (**6e**) resulted in a slight red shift in absorption to 268 nm, with no significant change to its emission maximum at 409 nm. However, **6e** displayed enhanced fluorescence intensity across a broader emission range compared to **6d**. Aminophenanthrene **6g**, bearing a phenyl substituent at the 6-position, showed a blue shifted absorption maximum at 256 nm and a markedly blue-shifted emission maximum at 348 nm.

A distinct trend was observed for hydroxyphenanthrene analogs **7d**, **7e**, and **7g** (Fig. 2B). Compound **7d** exhibited absorption and emission maxima at 265 and 378 nm, respectively. The methoxy-substituted analog **7e** demonstrated a similar absorption maximum (266 nm) but a significant red shift in emission maximum at 405 nm. Phenyl-substituted **7g** demonstrated modest red shifts to both absorption (275 nm) and emission (386 nm) maxima compared to **7d**.

Collectively, these results demonstrate that the fluorescence properties of amino- and hydroxyphenanthrene derivatives can be tuned through strategic substitution enabled by our method.

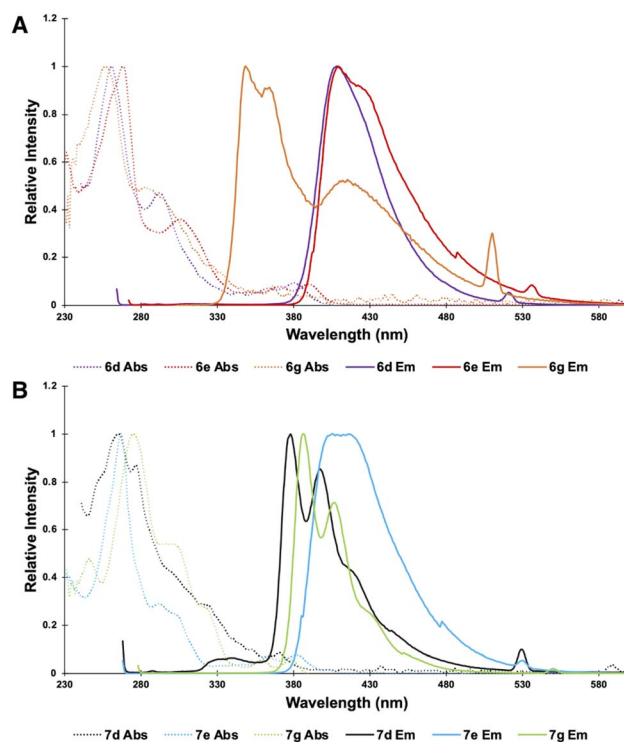


Fig. 2 Absorption (dotted) and emission (solid) spectra for (A) aminophenanthrenes **6d** (purple), **6e** (red), and **6g** (orange) and (B) hydroxyphenanthrenes **7d** (black), **7e** (green), and **7g** (blue). Data were collected at 10<sup>-5</sup> M concentrations in dichloromethane. Excitation wavelengths for emission spectra of **6d**, **6e**, and **6g** were 261, 268, 255 nm, respectively. Excitation wavelengths for emission spectra of **7d**, **7e**, and **7g** were 265, 265, 275 nm, respectively.

This tunability highlights the potential utility of our strategy for the development of next-generation phenanthrene-based materials for optoelectronic, sensing, and imaging applications.

## Conclusions

We have developed a general, metal-free, and operationally simple two-step strategy for the synthesis of 1- and 4-substituted amino- and hydroxyphenanthrenes from 1- and 2-naphthaldehydes. The sequence combines an *E*-selective Wittig olefination with a regioselective Houben–Hoesch annulation, providing predictable site selectivity and broad functional group tolerance without the need for precious metal catalysts or elaborate starting materials. The chemodivergent method accommodates diverse substitution patterns, enabling rapid scaffold diversification.

Beyond synthetic utility, we have demonstrated that substitutions introduced *via* this approach significantly influence the absorption and emission properties of the phenanthrene core. Methoxy and phenyl substituents, which extend pi conjugation, were shown to modulate absorption and emission profiles, highlighting the capacity of this method to tune photophysical properties. This tunability underscores the potential of the described strategy as a versatile platform for the preparation of phenanthrene-based materials.

## Author contributions

H. E. O.: performed all experiments, wrote original manuscript draft; V. K. O.: project conceptualization, supervision, and manuscript editing.

## Conflicts of interest

There are no conflicts to declare.

## Data availability

The data underlying this study is available in the published article and the supplementary information (SI). Supplementary information: experimental details, characterization data, NMR spectra, and crystallographic data have been included as part of the Supplementary Information. Additional crystallographic data for compounds **6d** and **7f**. See DOI: <https://doi.org/10.1039/d5ra06485f>.

CCDC 2420502 and 2468044 contain the supplementary crystallographic data for this paper.<sup>36a,b</sup>

## Acknowledgements

The authors thank the University of Missouri for start-up funding support for V. K. O., the Mizzou Black Alumni Network (MBAN) for funding support for H. E. O., and Dr Stephen Kelley of the University of Missouri Elmer O. Schlemper X-ray Diffraction Center for X-ray analyses.

## References

- S. E. John, R. Tokala, V. R. Kaki and N. Shankaraiah, *Asian J. Org. Chem.*, 2021, **10**, 2105.
- F.-W. Yan, C.-H. Chang, US Patent US20180301631A1, 2018.
- S. Wang, X. Yan, Z. Cheng, H. Zhang, Y. Liu and Y. Wang, *Angew. Chem., Int. Ed.*, 2015, **54**, 13068.
- R. X.-F. Ren, N. C. Chaudhuri, P. L. Paris, S. Rumney IV and E. T. Kool, *J. Am. Chem. Soc.*, 1996, **118**, 7671.
- P. Srivastava, P. C. Fürstenwerth, J. F. Witte and U. Resch-Genger, *New J. Chem.*, 2021, **45**, 13755.
- T. Xu, X. Yin, C. Zhai, D. Chen, X. Yang, S. Hu, K. Hu, Y. Shang, J. Dong, Z. Yao, Q. Li, P. Wang, R. Liu, M. Yao and B. Liu, *Chem. Sci.*, 2023, **14**, 11629.
- L. Wang, R.-J. Chen, J.-F. Yan and Y.-F. Yuan, *New J. Chem.*, 2023, **47**, 16129.
- H.-X. Nie, B. Zhang, Y.-M. Liu, M.-H. Yu and Z. Chang, *Inorg. Chem. Front.*, 2023, **10**, 6229.
- Q. H. Tran, X. Wang, M. Brookhart and O. Daugulis, *Organometallics*, 2020, **39**, 4704.
- Y. Wang, H. Ren, Y. Gao, S. He, S. Ni, G. Yang, R. Zhang, X. Zhao, W. Wu, L. Ma, Patent CN117700585A, 2024.
- D. Zhang, J. Guo, M. Zhang, X. Liu, M. Ba, X. Tao, L. Yu, Y. Guo and J. Dai, *J. Nat. Prod.*, 2017, **80**, 3241.
- X.-M. Zhou, C.-J. Zheng, L.-S. Gan, G.-Y. Chen, X.-P. Zhang, X.-P. Song, G.-N. Li and C.-G. Sun, *J. Nat. Prod.*, 2016, **79**, 1791.
- K. Machida, T. Abe, D. Arai, M. Okamoto, I. Shimizu, N. J. de Voogd, N. Fusetani and Y. Nakao, *Org. Lett.*, 2014, **16**, 1539.
- Y. Wang, S.-H. Guan, Y.-H. Meng, Y.-B. Zhang, C.-R. Cheng, Y.-Y. Shi, R.-H. Feng, F. Zheng, Z.-Y. Wu, J.-X. Zhang, M. Yang, X. Liu, Q. Li, X.-H. Chen, K.-S. Bi and D.-A. Guo, *Phytochemistry*, 2013, **94**, 268.
- W.-P. Hu, G.-D. Cao, J.-H. Zhu, J. Z. Li and X.-H. Liu, *RSC Adv.*, 2015, **5**, 82153.
- Y.-P. Liu, T.-W. Wang, Z. Xie, Y. Bian, Y.-Y. Liu, R.-Q. Guan, Z.-Y. Liu, L. Qiang, G.-Y. Chen and Y.-H. Fu, *J. Nat. Prod.*, 2021, **84**, 3117.
- Y. Liu, Z. Du, C. Sheng, G. Zhang, S. Yan, Z. Zhang and S. Qin, *Molecules*, 2025, **30**, 1204.
- W. M. Seganish and P. DeShong, *Org. Lett.*, 2006, **8**, 3951.
- C. P. Roy, S. Karmakar and J. Dash, *J. Org. Chem.*, 2024, **89**, 10511.
- P. Quinodoz, A. Kolleth, D. Dagonneau, M. Yoshimura, L. R. Méndez, M. Joigneaux, R. Staiger, R. Horber, S. Sulzer-Mossé, A. B. Cesaretli, U. K. Yezer, S. Catak and A. De Mesmaeker, *Helv. Chim. Acta*, 2022, **105**, e202200093.
- M. Yoshimura, P. Quinodoz, L. R. Méndez, A. Kolleth, S. Sulzer-Mossé, T. Vent-Schmidt, U. K. Yezer, S. Catak and A. De Mesmaeker, *Helv. Chim. Acta*, 2023, **106**, e202300085.
- T. Yao, M. A. Campo and R. C. Larock, *Org. Lett.*, 2004, **6**, 2677.
- T. Yao, M. A. Campo and R. C. Larock, *J. Org. Chem.*, 2005, **70**, 3511.
- Y. Kuninobu, T. Tatsuzaki, T. Matsuki and K. Takai, *J. Org. Chem.*, 2011, **76**, 7005.
- M. Murai, N. Hosokawa, D. Roy and K. Takai, *Org. Lett.*, 2014, **16**, 4134.
- R. Wakabayashi, T. Kurahashi and S. Matsubara, *Synlett*, 2013, **24**, 2297.
- V. Mamane, P. Hannen and A. Fürstner, *Chem.-Eur. J.*, 2004, **10**, 4556.
- S. M. Abdel-Wahhab, L. S. El-Assal, N. Ramses and A. H. Shehab, *J. Chem. Soc.*, 1968, 863–866.
- B.-B. Gou, H. Yang, H.-R. Sun, J. Chen, J. Wu and L. Zhou, *Org. Lett.*, 2019, **21**, 80.
- V. K. Outlaw and C. A. Townsend, *Org. Lett.*, 2014, **16**, 6334.
- H. E. Ozomari, K. T. Sharpe and V. K. Outlaw, *J. Org. Chem.*, 2024, **89**, 1310.
- J. Poater, R. Visser, M. Solà and F. M. Bickelhaupt, *J. Org. Chem.*, 2007, **72**, 1134.
- Y. Nagano, *J. Chem. Thermodyn.*, 2002, **34**, 377.
- R. Kalescky, E. Kraka and D. Cremer, *J. Phys. Chem. A*, 2014, **118**, 223.
- G. Portella, J. Poater and M. Solà, *J. Phys. Org. Chem.*, 2005, **18**, 785.
- (a) CCDC 2420502: Experimental Crystal Structure Determination, 2025, DOI: [10.5517/ccdc.csd.cc2m7qqb](https://doi.org/10.5517/ccdc.csd.cc2m7qqb); (b) CCDC 2468044: Experimental Crystal Structure Determination, 2025, DOI: [10.5517/ccdc.csd.cc2nv6b2](https://doi.org/10.5517/ccdc.csd.cc2nv6b2).

